

## Searching for UHE photons in the EeV range: a two-variable approach exploiting air-shower universality.

---

**Pierpaolo Savina\***, Carla Bleve, Lorenzo Perrone

*Università del Salento, INFN sezione di Lecce,*

*E-mail: [pierpaolo.savina@le.infn.it](mailto:pierpaolo.savina@le.infn.it)*

The signatures of a photon-induced air shower are a larger atmospheric depth at the shower maximum ( $X_{\max}$ ) and a lower number of muons with respect to the bulk of hadron-induced background. Hybrid experiments combining a fluorescence detector (FD) and a ground array of particle detectors (SD) can measure  $X_{\max}$ , energy ( $E$ ) and the geometry of the shower with high precision. The muonic content is usually estimated through mass-sensitive SD observables that have a complex dependence on the shower geometry,  $E$  and  $X_{\max}$ . We present here a method to simplify this approach using the paradigm of universality. Air-shower universality models the average contribution of different secondary particles starting from a limited number of parameters such as  $E$ ,  $X_{\max}$ , the muonic content and the geometrical configuration of the shower axis relative to the detector. We describe a method to derive a parameter,  $R_{\mu}$ , directly related to the muonic content using the total signal recorded in individual detectors of a ground array. The approach is tested on full air shower simulations using as a case study the array of water-Cherenkov detectors of the Pierre Auger Observatory. The technique is explored in terms of photon/hadron separation capability over the energy range between 1 and 30 EeV. We show how the combination of  $R_{\mu}$  and  $X_{\max}$ , in the case of hybrid detection, can lead to a strong hadron/photon separation power even when the number of triggered stations at the ground is limited.

*36th International Cosmic Ray Conference -ICRC2019-  
July 24th - August 1st, 2019  
Madison, WI, U.S.A.*

---

\*Speaker.

## 1. Introduction

Photons with energies larger than  $10^{18}$  eV (UHE-photons) are important to reveal the origin of cosmic rays of the highest energy. Nuclei from sources are expected to produce a flux of UHE-photons interacting with the extra-galactic background light during their propagation. This cosmogenic flux depends on the characteristics and distribution of the sources. Thus, observing UHE-photons, can pose constraints on the cosmic rays origin and properties of the sources.

Since the cosmogenic flux integrated above  $10^{18}$  eV is less than  $0.027 \text{ km}^{-2} \text{ sr}^{-1} \text{ yr}^{-1}$  [1] the search for UHE-photons requires large effective areas that can be achieved only with ground-based detectors of extensive air showers (EAS) like the Pierre Auger Observatory or Telescope Array [1–4] with instrumented areas of hundreds of  $\text{km}^2$ . The identification of photon primaries, when EAS detectors are used, relies on the ability to distinguish between the signal and the overwhelming background due to the showers initiated by nuclei.

Since the radiation length is more than two orders of magnitude smaller than the mean free path for photo-nuclear interaction, in photon showers the transfer of energy to the hadron/muon channel is reduced with respect to the bulk of hadron-induced air showers, resulting in a lower number of muons ( $N_\mu$ ). Additionally, as the development of photon showers is delayed by the typically small multiplicity of electromagnetic interactions, they reach the maximum development of the shower ( $X_{\text{max}}$ ) deeper in the atmosphere with respect to showers initiated by hadrons (fig. 1).

Hybrid detectors of EAS like the Pierre Auger Observatory or Telescope Array combine a Fluorescence Detector (FD) capable of measuring the longitudinal development of a shower and an array of particle detectors (SD) sampling secondary shower particles at ground level. The FD can directly access  $X_{\text{max}}$ ,  $N_\mu$  instead is not directly measured and is accounted for only through mass-sensitive SD observables that have a complex dependence on  $N_\mu$ , but also on the shower geometry, energy and  $X_{\text{max}}$  [1, 2].

In this work, using the concept of air-shower universality, we introduce a parameter,  $R_\mu$ , directly related to the muonic content of the shower, to be used as a proxy for  $N_\mu$  along with  $X_{\text{max}}$  to search for photons above  $10^{18}$  eV. The parameter is defined in section 2, and studied in section 3 using events simulated with the Pierre Auger Observatory detector configuration. Finally, in section 4, we show the discrimination power between photon and hadron air shower simulations when only  $X_{\text{max}}$  and  $R_\mu$  are used.

## 2. Universality and relative muon content

A high energy cosmic ray that hits the atmosphere produces a large number of secondary particles, (e.g. a proton shower with energy of  $10^{19}$  eV, about  $10^{10}$  particles reach the ground). The shower particles can be treated as a “thermodynamic” system, that can be described with a few parameters. This property of cosmic rays is known as “universality” [5].

For purely electromagnetic cascades the lateral and longitudinal development along with the distribution of secondary particles in energy and angle, depends only on the energy of the primary and the stage of development of the shower. This concept can be extended to hadronic cascades by introducing an additional parameter ( $R_\mu$ ), related to the muonic content of the shower [6].

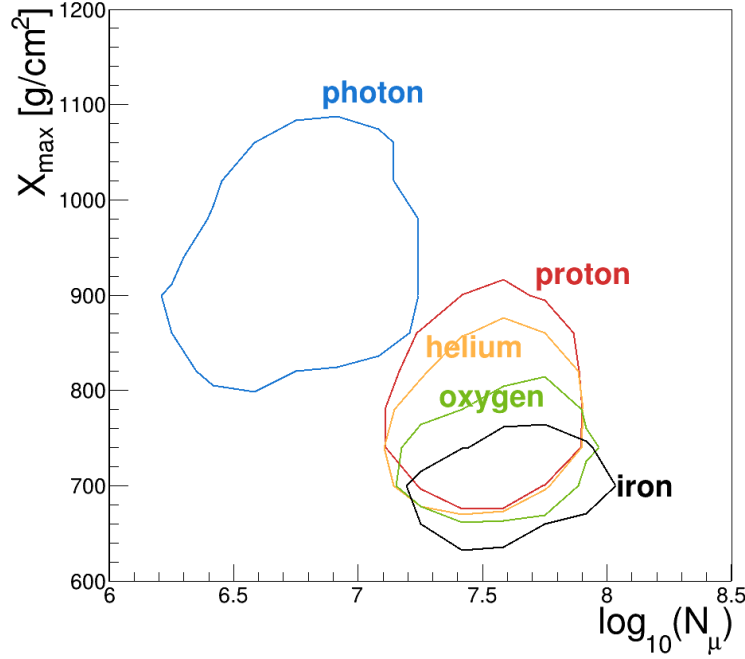


**Figure 1:**  $X_{max}$  and  $N_{\mu}$  distributions for air-shower initiated by different primaries, with an energy ranging between  $10^{18.5}$  eV and  $10^{19.0}$  eV. Contour lines enclose the 90% of the distribution for each primary type. Photon-initiated showers are well separated from showers initiated by hadrons.

In [7] it is shown that any air shower can be described as the superposition of four different components:  $e^{\pm}$  and  $\gamma$  from high energy  $\pi^0$ ; muons;  $e^{\pm}$  and  $\gamma$  from muon decays;  $e^{\pm}$  and  $\gamma$  from hadronic interactions at low energies. Each component has a universal behaviour depending only on the energy and stage of development of the shower. The contributions of the four components, instead, depend on the mass of the primary particle, through a single parameter representing the total number of muons in the shower. As a consequence, it is possible to develop a model that predicts the average value of the signal measured at ground with a particle detector, for any kind of detector used in the array. A parametrization of each component was derived in [7] for the water-Cherenkov detectors of the Pierre Auger Observatory using QGSJetII-03 proton simulations. For any primary and hadronic model the predicted total signal can be expressed as in the following, with  $i$  running over the four components:

$$S_{\text{pred}} = \sum_{i=1}^4 S_i = \sum_{i=1}^4 \beta_i(R_{\mu}) \cdot S_i^{\text{ref}} \quad (2.1)$$

$S_i^{\text{ref}}$  parametrized is the reference signal [7] depending on energy,  $X_{max}$ , and geometry. The mass dependence is entirely contained in the coefficients  $\beta_i$  and  $R_{\mu} = S_{\mu}/S_{\mu}^{\text{ref}}$  is the muonic signal relative to the predicted average value. For the pure muonic component  $\beta_{\mu}(R_{\mu}) = R_{\mu}$ . Given the observed signal  $S_{\text{obs}}$  in an individual detector,  $R_{\mu}$  can be estimated requiring  $S_{\text{obs}} = S_{\text{pred}}$  in equation 2.1 and solving for  $R_{\mu}$ . The functional form of  $\beta_i(R_{\mu})$  are taken from [7].

In the next section this method for reconstructing  $R_{\mu}$  will be applied to realistic simulations of a hybrid detector with the Pierre Auger Observatory configuration.

### 3. $R_\mu$ as mass composition parameter: simulation study

As photon-initiated showers develop as an almost pure electromagnetic cascade, they are characterized by a much smaller muonic content with respect to hadronic showers leading to a large expected differences in  $R_\mu$ .

For studying the  $R_\mu$  distribution we use a shower library simulated with CORSIKA [8] using EPOS-LHC [9] as high-energy hadronic interaction model. Showers initiated by photons and protons are simulated in an energy range from  $10^{17.5}$  eV to  $10^{19.5}$  eV according to a power law spectrum  $E^{-\gamma}$  with  $\gamma = 1.0$  and zenith angle from  $0^\circ$  to  $65^\circ$ . Realistic simulations of a hybrid detector with the same configuration of the Pierre Auger Observatory [10] are then performed [11]. The resulting hybrid events are reconstructed following [10]. Selection criteria similar to [1] are applied to ensure a good geometry and longitudinal profile reconstruction. Only showers with reconstructed zenith  $\theta < 60^\circ$  are considered in the following.

Since the true value of  $S_\mu$  is available in simulations, we can obtain  $R_\mu^{\text{MC}} = S_\mu/S_\mu^{\text{ref}}$ . We observe that the mean values for EPOS-LHC are remarkably constant in  $E$  and  $\theta$ , and are  $\sim 1.3$  for protons and  $\sim 0.3$  for photons (see fig. 3 dark blue histograms). This means that the dependence on the number of muons on  $E$  and  $\theta$  is approximately the same for QGSJetII-03 and EPOS-LHC and that they only differ for an overall scale factor. We now aim at verifying that the  $R_\mu$  reconstruction method does not introduce any bias with respect to  $R_\mu^{\text{MC}}$ . Using simulated proton events selected as explained above, we study the performance of the  $R_\mu$  reconstruction as a function of the signal

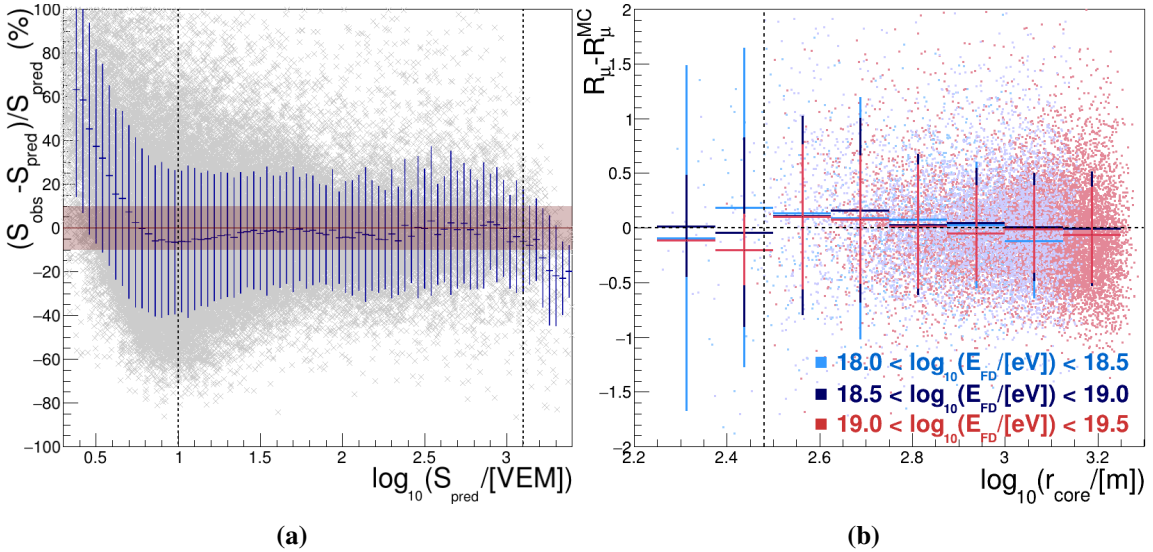


**Figure 2:** Check for biases due to detector effects on the universal description of the total signal in the case of EPOS-LHC protons in the  $10^{18.0} - 10^{19.5}$  eV range. (a) relative difference between the predicted and observed signal. Between 10 VEM and 1250 VEM the accuracy of the parametrization is better than 10% (red band). Trigger (left) or saturation (right) effects are visible outside the region enclosed by the dash lines. (b) difference between the calculated and the true  $R_\mu$  as a function of the core distance. Vertical bars represent the standard deviation of the distribution in each bin for both plots.

and the radial distance from the shower axis for individual SD detectors.

In fig. 2a the relative difference between the observed and the predicted signal is shown as a function of the predicted signal in individual stations, calculated using 2.1 with the true value of  $R_\mu$ . For signals between 10 VEM<sup>1</sup> and 1250 VEM, the accuracy of the model prediction is better than 10% (red band). For smaller (larger) signals, trigger (saturation) effects truncate the distribution on one side producing a visible bias.

In fig. 2b the difference between the reconstructed and the true value of the relative muon content is shown as a function of the distance from the shower axis. The reconstruction of  $R_\mu$  does not present any significant bias. Due to the steepness of the lateral distribution close to the axis, we decided not to use small distances to avoid the total signal prediction being strongly affected by the resolution on the core reconstruction. Hence we require  $10 \text{ VEM} < S_{\text{pred}} < 1250 \text{ VEM}$  and  $r > 300 \text{ m}$  (black dashed lines) for further applications of the  $R_\mu$  reconstruction.

To obtain an event-wise estimate of the muon content, the average  $R_\mu$  of the selected station is assigned to an event if more than one station is available<sup>2</sup>.

In fig. 3 the resolution of the reconstruction method is presented for protons (left) and photons (right). The  $R_\mu$  distribution is shown at different levels:  $R_\mu^{\text{MC}}$  (dark blue) is the Monte Carlo value,  $R_\mu^{\text{Exp}}$  (light blue) is the value reconstructed using as input for the model the true values of energy,  $X_{\text{max}}$  and geometry, while for  $R_\mu^{\text{FD Rec}}$  (red) hybrid reconstructed values are used. For a given primary, all distributions have the same mean values thus proving that the reconstruction method is unbiased. The spread of  $R_\mu^{\text{MC}}$  is mainly due to the shower to shower fluctuations. For  $R_\mu^{\text{Exp}}$  we also

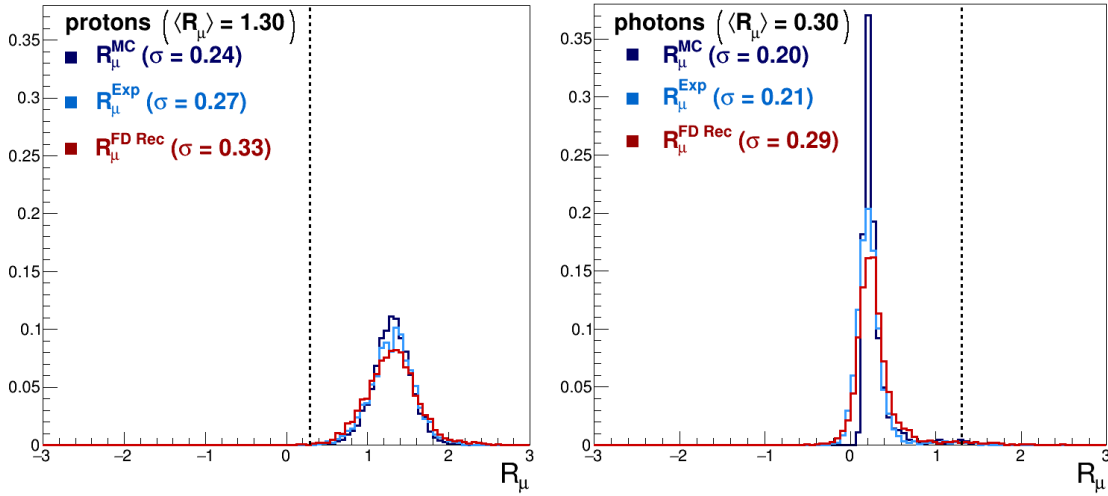


**Figure 3:**  $R_\mu$  distributions for protons (left) and photons (right) primaries. In dark blue the distribution of the Monte Carlo value of  $R_\mu$ . In light blue the distribution of  $R_\mu$  reconstructed with the true values of energy,  $X_{\text{max}}$  and geometry as input for  $S_{\text{pred}}$ . In red the distribution of  $R_\mu$  when the hybrid reconstructed values are used (realistic case). Dashed black lines represent the mean value of  $R_\mu$  for the other primary type.

<sup>1</sup>Signals are expressed in Vertical Equivalent Muon (VEM) units, i.e. the mean signal produced from a vertical muon in a WCD of the Pierre Auger Observatory [10].

<sup>2</sup>The minimum required number of stations for the  $R_\mu$  reconstruction is one.

have sampling fluctuations and in the  $R_\mu^{\text{FD Rec}}$  distribution we observe additionally the effects of the resolution of the hybrid reconstruction.

Photon and proton distributions can be easily compared through the dashed black lines, that show the mean value of the distribution of the other primary type considered and are in both cases at more than  $3\sigma$  from the mean.

#### 4. Search for photons

In this section we introduce a method to search for photon primaries in hybrid data, based on a two-variable approach.  $R_\mu$  and  $X_{\text{max}}$  are used, as they have a clear physical meaning and a strong relation to the nature of primary particles. For each event  $X_{\text{max}}$  is directly provided by the hybrid reconstruction, while  $R_\mu$  is calculated as described in the previous sections.

For studying the separation power of the two variables we use simulations of photon signal and of proton background.

In fig. 4 the distributions of  $R_\mu$  and  $X_{\text{max}}$  are shown for photons (blue) and protons (red) in the energy range  $10^{18}$ – $10^{19.5}$  eV. As expected,  $X_{\text{max}}-R_\mu$  resembles the  $X_{\text{max}}-N_\mu$  distribution of fig. 1 with two clearly separated central peaks and minimal overlap of the tails.

To identify a photon signal against the proton background, a Fisher Analysis is used with  $R_\mu$ ,  $X_{\text{max}}$  and energy as input parameters. The energy is used in the Fisher Analysis to take into account

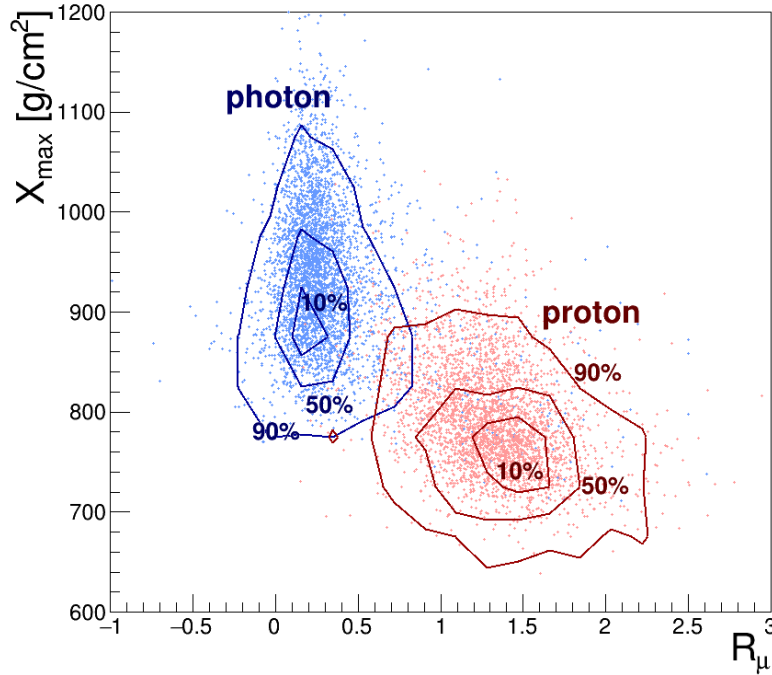


**Figure 4:**  $(X_{\text{max}}, R_\mu)$  distributions for photons (blue) and protons (red) in a energy range  $10^{18}$ – $10^{19.5}$  eV. Signal and background are well separated with a minimal overlapping area. Contour lines enclose the 90%, 50% and 10% of the distributions of events weighted to a realistic power law spectrum  $E^{-\gamma}$  with  $\gamma = 2.7$  for proton background and  $\gamma = 2.0$  for photons, while the underlying scatter plot refers to unweighted  $E^{-1.0}$  spectrum used for simulations.

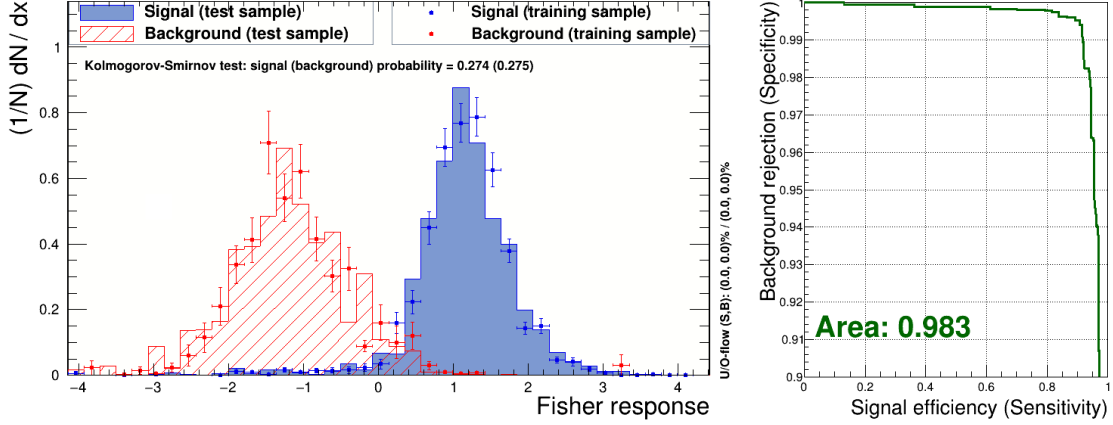


**Figure 5:** On the left: Fisher response of the TMVA analysis performed using  $R_\mu$ ,  $X_{\max}$  and energy as separation parameters, for photon (signal, blue) and proton (background, red) primaries; on the right: Relative Operating Characteristic (ROC) curve of the analysis that shows the background rejection vs signal efficiency.

the energy dependence of  $X_{\max}$ . The training and testing is done using TMVA [13] with simulations reweighted to realistic spectra ( $E^{-\gamma}$  with  $\gamma = 2.7$  for protons and  $\gamma = 2.0$  for photons).

In fig. 5 left the resulting Fisher response distributions are shown for photons (blue) and protons (red). As shown in fig. 5 right, the background rejection is found to be around 99.90% for signal efficiency of 50% used as *a priori* choice in [1]. Still a very good background rejection (99.50%) is found with a much less conservative choice of a candidate cut that corresponds to a signal efficiency of 90%.

Proton-initiated showers induce the highest contamination of the signal distribution (see fig. 1), therefore an even better separation is expected in data, where the composition is heavier than pure protons [14].

## 5. Conclusions

In this work we discussed a new method for the search of photon primaries in the EeV range using hybrid detectors.  $X_{\max}$  and  $R_\mu$  are two parameters related to the nature of a primary particle that can be used to separate photon-initiated showers from hadronic showers.

We have shown that, while  $X_{\max}$  is directly measured by the FD, the relative muon content  $R_\mu$  can be estimated through universality techniques, using the signal recorded by the SD. We have defined the minimum requirements for an unbiased reconstruction of  $R_\mu$  when using the reconstructed values of energy,  $X_{\max}$  and geometry provided by FD.

Finally we reported the results of the photon-hadron separation using a Fisher discrimination analysis performed on simulations of photon and proton induced showers. For a signal efficiency of 90% the background rejection is 99.50% for realistic signal and background energy spectra. This separation power derived for a pure proton background is expected to be enhanced in data because of the mass composition of cosmic rays. A future goal is to explore the potential of this analysis

with hybrid data of the Pierre Auger Observatory. Based on the argument discussed in this work we then expect a positive impact on the current upper limits on the photon flux in the EeV range.

## 6. Acknowledgments

We are very grateful to the Pierre Auger Collaboration for providing the software and the CORSIKA simulation library used in this work. In particular we are thankful to the photon analysis working group and to Marcus Niechciol, Markus Risse and Markus Roth for their constructive suggestions and support.

## References

- [1] The Pierre Auger Collaboration, JCAP **04** (2017) 009;
- [2] Telescope Array Collaboration, Astropart.Phys. **110** (2019) 8-14;
- [3] The Pierre Auger Collaboration, PoS ICRC2015 (2016) 1103;
- [4] The Pierre Auger Collaboration, Astropart.Phys **29** (2008) 243-256;
- [5] P. Lipari, Phys. Rev. **79** (2008) 063001;
- [6] F. Nerling, J. Blumer, R. Engel, M. Risse, Astropart. Phys. **24** (2006) 421-437;
- [7] M. Ave, R. Engel, M. Roth, A. Schulz, Astropart. Phys. **87** (2017) 23-39;
- [8] D.Heck, J. Knapp, J. Capdevielle, G. Schatz, T. Thouw, Wissenschaftliche Berichte, Forschungszentrum Karlsruhe FZKA 6019 (1998);
- [9] T. Pierog, Iu. Karpenko, J. M. Katzy, E. Yatsenko, and K. Werner, Phys. Rev. **C92** (2015) 034906;
- [10] The Pierre Auger Collaboration, Nucl. Instrum. Meth. **A798** (2015) 172-213;
- [11] S. Argiro, et al. Nucl. Instrum. Meth. **A580** (2007) 1485-1496;
- [12] R. A. Fisher, Annals Eugenics **7** (1936) 7;
- [13] A. Hoecker, et al. PoS A CAT **040** (2007);
- [14] The Pierre Auger Collaboration, Physical Review D **90** (2014) 122006.